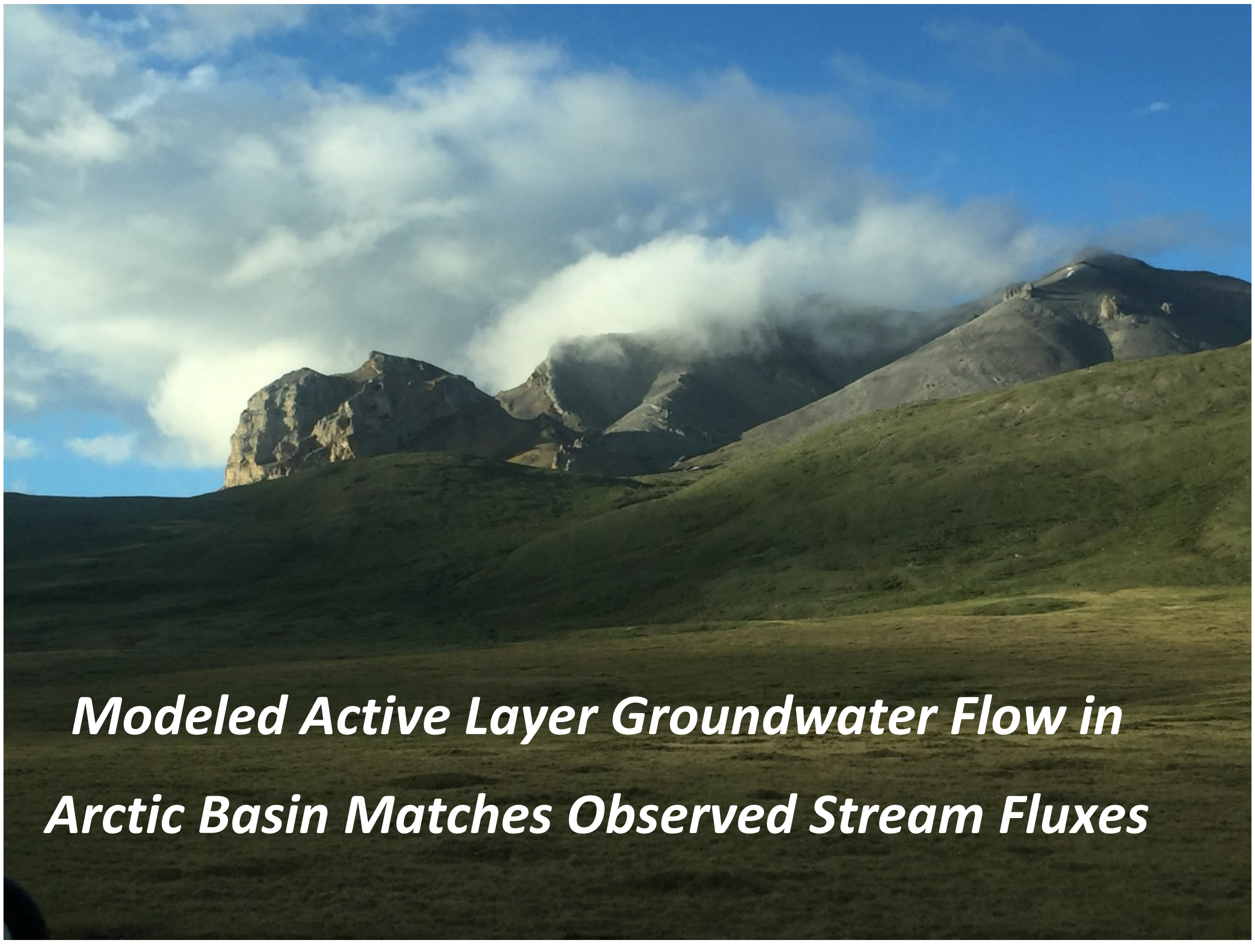

Kindra Nicholaides

Jackson School of Geosciences, University of Texas at Austin

Introduction

As global temperatures climb, the Arctic latitudes are affected most acutely; warming here will be 2 to 3 times greater than in tropical zones (Kane et al., 1991). We are seeing reduced mass of glaciers, earlier occurring snow melts, and greater overall variability in weather (Hinzman et al. 2005). Permafrost temperatures have been observed to be 2°C warmer than 20 to 30 years ago (Romanovsky et al., 2010) with increased thaw depth that is expected to continue to increase by over 50% of current depths (Walsh et al., 2005).

The active layer is the seasonally thawed bed of soil from the ground surface to the top of the ice table and the location of essential hydrological, biological and chemical processes (Kane et al., 1991)(see Figure 1). When permafrost melts and the base of the active layer deepens, its store of frozen organic carbon is exposed to aerobic conditions. The organic carbon can be microbially metabolized (Capek et al. 2015) and released into the atmosphere as greenhouse gases, CO_2 and CH_4 (Shuur et al., 2008). Estimated to house nearly 50% of the global organic carbon, the Alaskan coastal plain has transitioned from a net sink to a net source of CO_2 for the atmosphere (Oechel et al., 2000). This is a positive feedback loop with potentially important implications for global warming (Shuur et al., 2008).

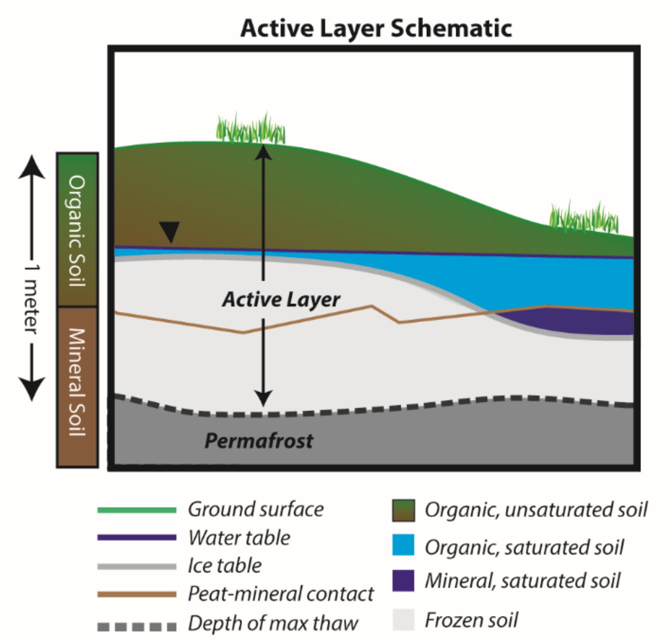

Figure 1 Active layer diagram

Since the 1990s it has been predicted that permafrost would degrade due to increasing surface temperatures and that increase in active layer thickness would be proportional to the rise in temperature (Kane et al., 1991; Hinzman and Kane, 1992). Subsequent permafrost degradation has been documented in areas of discontinuous permafrost. From studies in Healy, Alaska, Osterkamp and Romanovsky (1999) reported increased thawing of the active layer and formation of new taliks, which are thaw spots in permafrost that link to regional groundwater flow. Jorgenson et al. (2006) documented the degradation of ice wedges and formation of thermokarst in Northern Alaska through small scale field studies and large scale aerial time-series photograph comparison from 1945, 1982, and 2001. They correlated this melting to a slight increase in ground temperature. Between 1995 and 2000, Hinkel and Nelson (2003) found a correlation between maximum thaw and local air temperatures at seven sites on the Alaskan North Slope. More recently, Muskett and Romanovsky (2011) used GRACE satellite and runoff data to calculate the increase in groundwater storage in the Alaskan Arctic coastal plain from 1999 to 2009. They hypothesized this was due to increased active layer thickness below thaw rivers and lakes.

The deepening of the active layer is likely to increase groundwater fluxes. The Arctic has been generally considered a surface water dominated system and so few studies or models have attempted to incorporate groundwater models. Previous flow models such as TOPMODEL, ARRHYTHM, and Topoflow have been applied to arctic basin flow but none of them take into account the extreme spatial and temporal variability of active layer hydraulic properties. Such variability has the potential to dominate groundwater fluxes.

Objective

Here I apply previously collected observational data from an arctic hillslope to a watershed-scope model of groundwater active layer flow. My goal is to determine if accurate base flow can be determined at a moment in time using only information derived from a digital elevation model and averaged transmissivity of the active layer. This technique disregards lateral heterogeneity of soils and vertically integrates what otherwise is an extremely variable vertical layer.

Site Description

Imnavait Creek Basin is a small watershed located on the northern foothills of the Brooks Range, on the Alaskan North Slope. It is a north-south trending stream valley with wet acidic tundra and visible water tracks over continuous permafrost (Hinkel and Nelson, 2003). The mineral soil is made of silt and glacial till (Kane et al., 1989). It is the site of many other environmental and arctic studies due to the Fairbanks Alaska University Research Station being located there. Kane et al. (1989) fully describes the hydrology of the site as well including the thickness of the active layer at max thaw of 40 cm without much internal variation. Since that paper was published, the active layer measurement data set I used is evidence of permafrost degradation in that site.

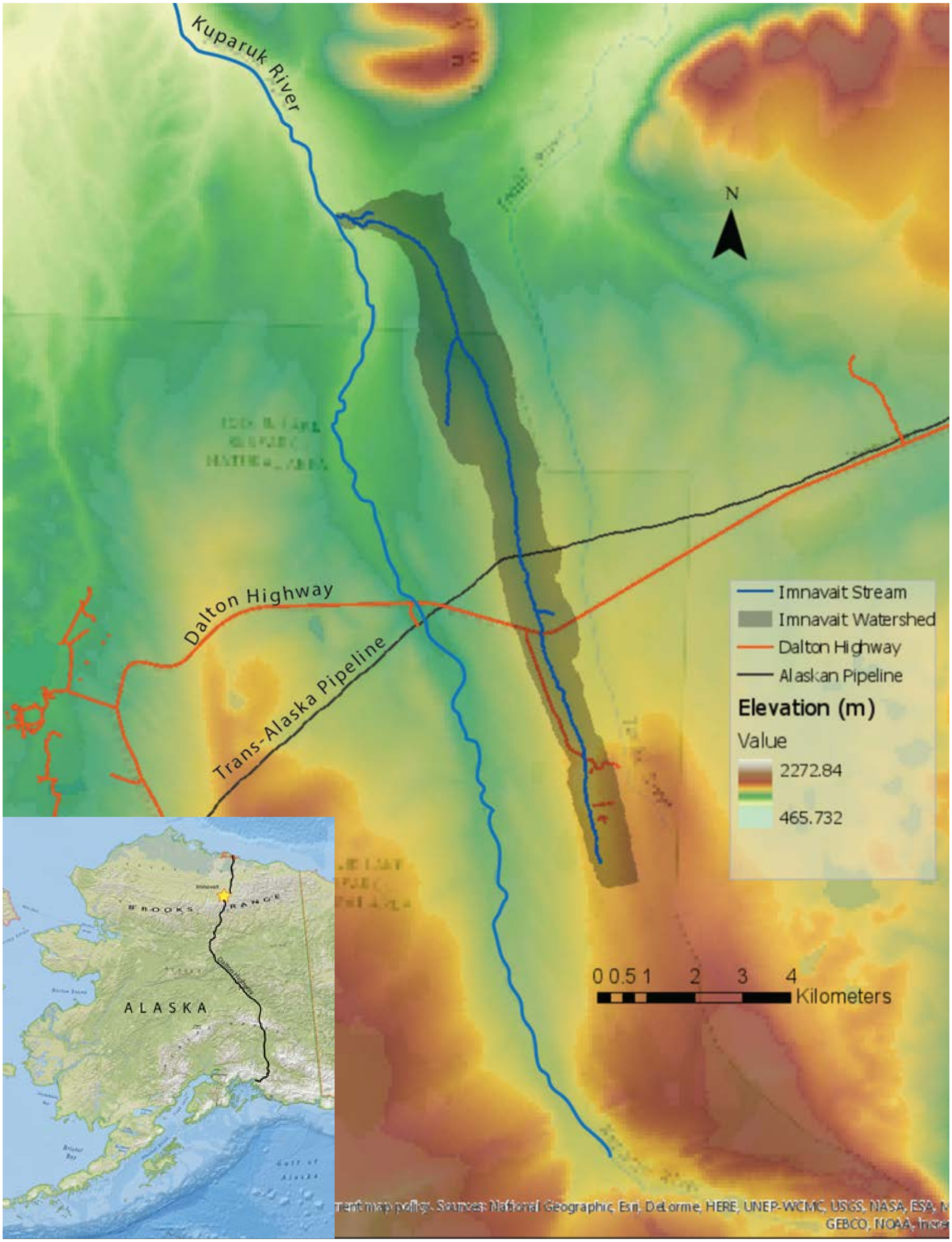

Figure 2 Map of Imnaviat watershed. Hydrograph data collected at confluence of Imnavait Creek and the Kuparuk River.

Figure 3. Imanvait is a beaded stream.

Methods

1. *Data collection and Preprocessing*

This project is entirely based on data collected by Mike O'Connor for his PhD thesis.

(a) Observational Data at hillslope site

On August 11, 2015 on a hillslope in Imanvait watershed, he installed 80 piezometers in a grid travelling 600 meters up slope, perpendicular to the stream (see Figure 4). At each well, he measured depth from ground surface to the water table and the depth to the ice table. Additionally he collectedsoil core sample within the grid at various depths in the active layer.

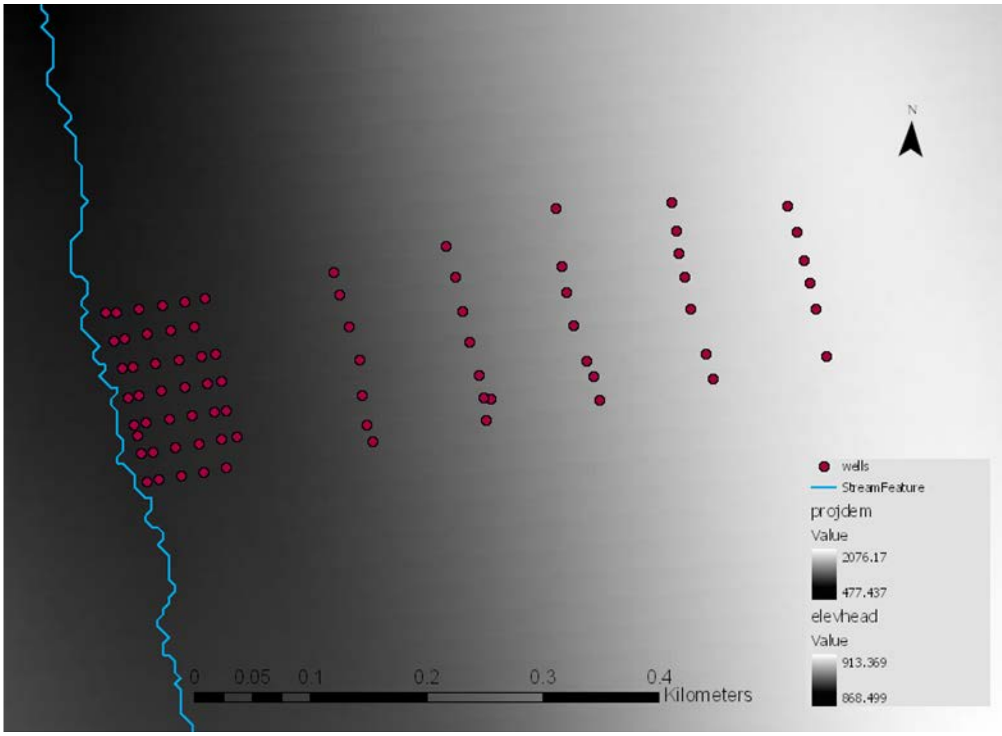

Figure 4 Grid of piezometers from stream to 600 meters up the hillslope

(b) Determine physical properties of soils

After running falling head tests on the soil cores, he was able to determine an empirical equation of hydraulic conductivity relative to depth for this hillslope. Using the depth to the water table and depth to ice table data, I determined the saturated thickness of the water table. I integrated the hydraulic conductivity over the range of saturated thickness using the following equation where z1 is the depth to the ice, z2 is the depth to the water and K(z) is the hydraulic conductivity as a function of depth:

$$\boldsymbol{T(z) = \int_{z1}^{z2} K dz}$$

I determined the transmissivity of the aquifer at each well on the hillslope.

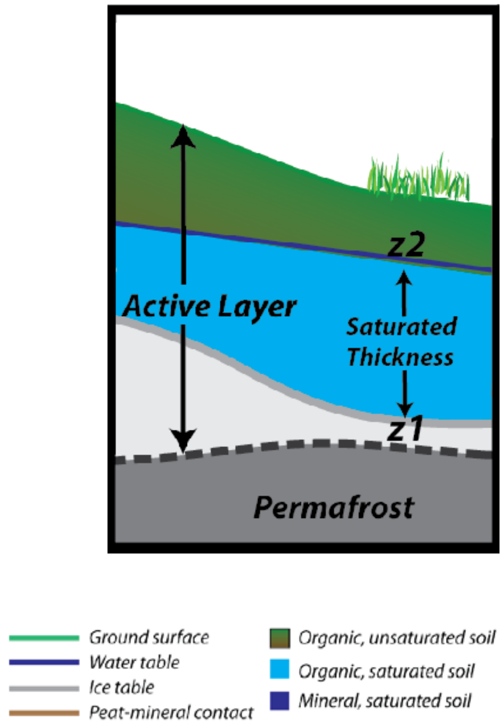

Figure 5. Saturated thickness is the distance from the ice table to the water table

(c) Digital Elevation Model

I downloaded a 5m DEM from the Polar Geospatial Center of the University of Minnesota. Their ArcticDEM Project is in the process of releasing high resolution maps of the entire Arctic. The spatial reference is GCS North American 1983 with a North American 1983 datum.

(d)Watershed and Stream Delineation

I imported my wells' GPS locations as XY data using UTM zone 6N projection. My excel sheet also contained depth data and the calculated transmissivity values . I delineated the watershed and the stream. I first filled the pits, then used the Flow Accumulation and Flow Direction tools. I created a pour point and used the watershed tool. I selected flow accumulations cells that had a value of greater than 500 in Raster Calculator and used the Stream Link tool, then Stream to Feature.

2. Inputs for Darcy Flow Tool

The Darcy Flow Tool uses Darcy's Law to calculate seepage velocity:

Based on **Darcy's Law**:

$$q = \frac{Q}{A} = -K\,\nabla h$$

q = darcy velocity [L/t]
K= hydraulic conductivity
h = hydraulic head
Q = discharge [L^3/t]
A = cross sectional area = width of rater cell (w) x height of saturated thickness (b)

Seepage velocity :

$$v = \frac{q}{n} = \frac{-T\nabla h}{bn}$$

T = transmissivity
b = saturated thickness
n = porosity

Therefore it makes sense that the Darcy Flow Tool requires four inputs (see Figure 6):

- Groundwater head elevation raster
- Porosity raster
- Saturated thickness raster
- Transmissivity raster

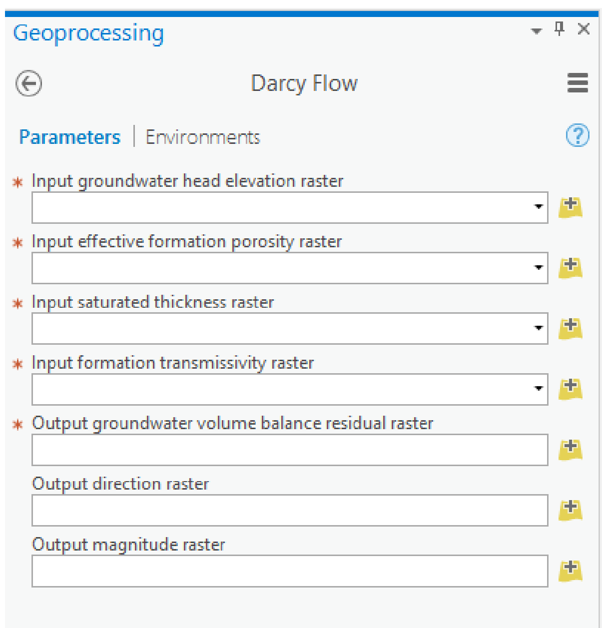

Figure 6. Darcy Flow tool GUI and the inputs/ outputs

Because my goal is discharge (Q) rather than seepage velocity, after using the Darcy Flow Tool, I undo some of the calculations of the tool by multiplying by porosity and then by saturated thickness and by the width of my raster. This way my end result raster is volume/time flux.

$$v = \frac{Q}{An} = \frac{-T\nabla h}{bn}$$

Let A = w * b

$$\frac{Q}{w * b * n} = \frac{-T\nabla h}{bn}$$

$$Q = \frac{-T\nabla h}{bn} * w * b * n$$

Note w = raster cell size, 5 m, and w and n cancel so their raster values are arbitrary.

Build Rasters from observational hillslope data and test run the Darcy Tool.

I used the Inverse Distance Weighting Tool (IDW) to create rasters based on my transmissivity data and depth to water table data. I create an elevation head by subtracting the depth to water table interpolated surface from the DEM. Running the Darcy Flow tool with these inputs, and a constant raster for porosity, resulted in a reasonable result. I then multiplied by the porosity raster and by 5 which is the width of my raster.

3. Determine hillslope characterization and apply to whole watershed

In order to find are relationship between the observational data and the hillslope, I compare the changing in slope % to how the extrapolated transmissivity raster changes with distance from stream. Using the slope tool, I created a slope raster of the hillslope extracted the slope values at the location of the piezometers (see Figure 7).

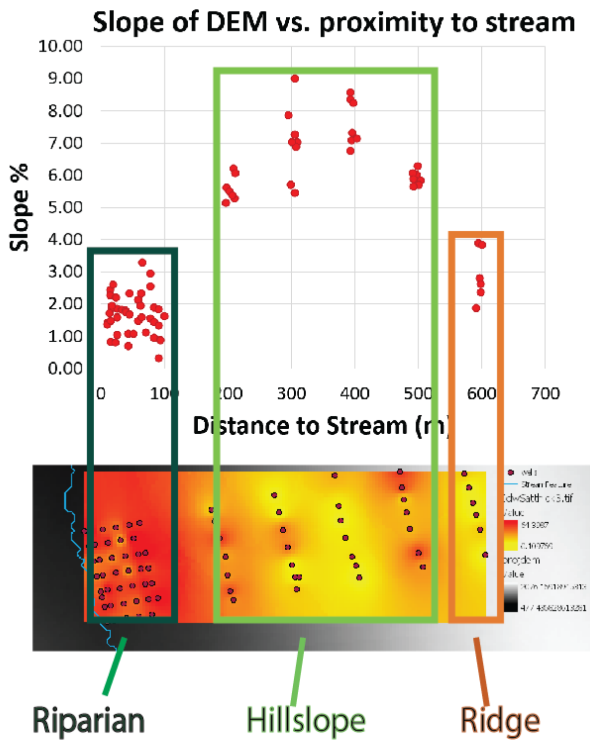

Figure 7. Plot of slope v. distance to the stream above extrapolated transmissivity raster on hillslope.

Both the transmissivity raster on the hillslope and the slope vs. distance from the stream can be divided into 3 zones. The Riparian Zone is within about 100m of the stream, has high relative transmissivity and has a slope of less than around 2.5%, the Hillslope Zone has lower transmissivity and a slope range from 3-9%, and the Ridge Zone has a slope of 4% and less.

Scaling Up

In order to apply this to the entire watershed I used Raster Calculator to select the cells with slopes less than 2.5% (see Figure 8). I delineated these values in the Riparian zone and repeated the process to delineate the Ridge zone. After I delineate these 2 zones (drawing polygons over the raster, turning polygons into rasters), I use the Mosaic tool to combine the 2 rasters with a constant value raster and I assigned each raster zone of the new mosaic a value 1-3.

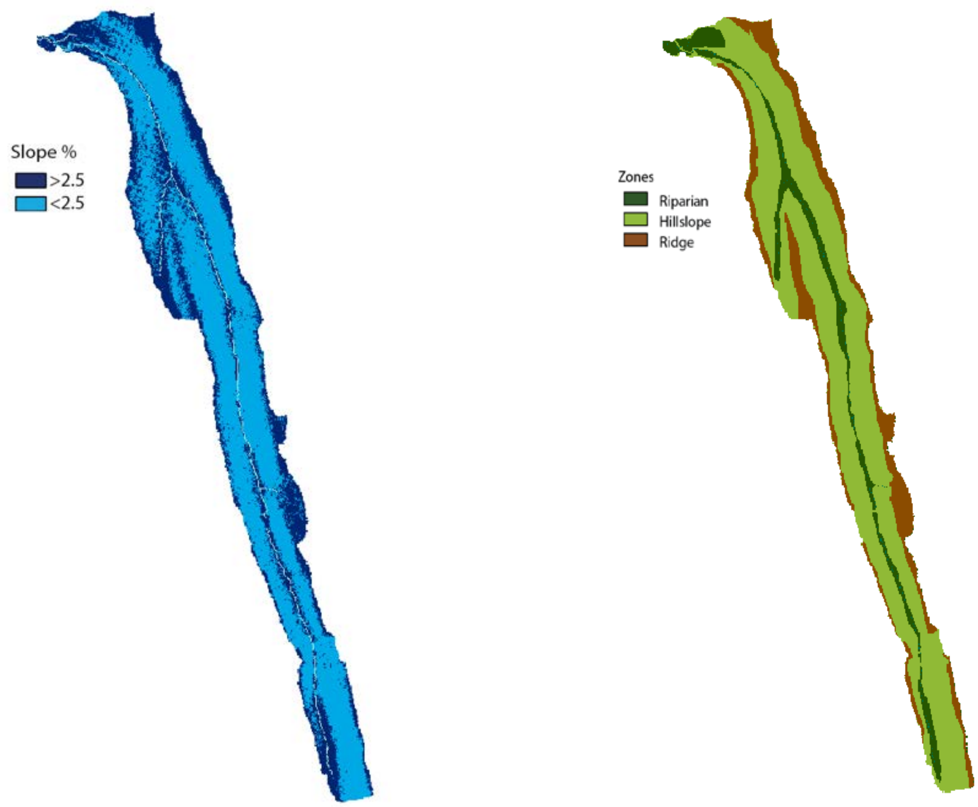

Figure 8. Left: Raster of watershed showing all cells with slope less than 2.5% occur in the riparian zone and the ridge. Right: Mosaic raster showing the 3 zones created within the watershed based on change in slope.

4. *Apply Darcy Flow Tool to whole Imnavait Basin*

Assign values to zoned template raster and use Darcy Flow Tool

For each of the 3 zones, I found a mean value of transmissivity and depth to water table.
Using the Mosaic raster as a template, I assigned each of the 3 zones a different transmissivity. I created another raster, assigning each zone the mean depth to water for that zone. From the Watershed DEM I subtracted the depth to water raster to create a water table elevation map which I used as my groundwater head elevation input. I used a constant raster for the porosity and the saturated thickness.

After applying the Darcy Flow Tool with these 4 inputs, I got a magnitude raster which I then multiplied by the Porosity raster and the constant raster as well as multiplying by 5, following the equation for discharge flux I derived earlier.

Calculate entire watershed flux with zoning tool
This tool calculates flow lines by summing up the flux in all the cells along a specific flow path. Any cell chosen in the raster will be the sum of all the previous fluxes along the flow path. In order to assess the

flux that is coming in to the stream from the entire watershed, it is necessary to sum all the cells on either side of the stream. I created a Multiple Ring Buffer at 5 and 10 meters around my stream feature. I deleted the middle section in editing mode and was left with a polygon ring around the entire stream (see Figure 9)

I used the Zonal Statistics tool to select and sum all the raster cells with which my stream buffer intersected.

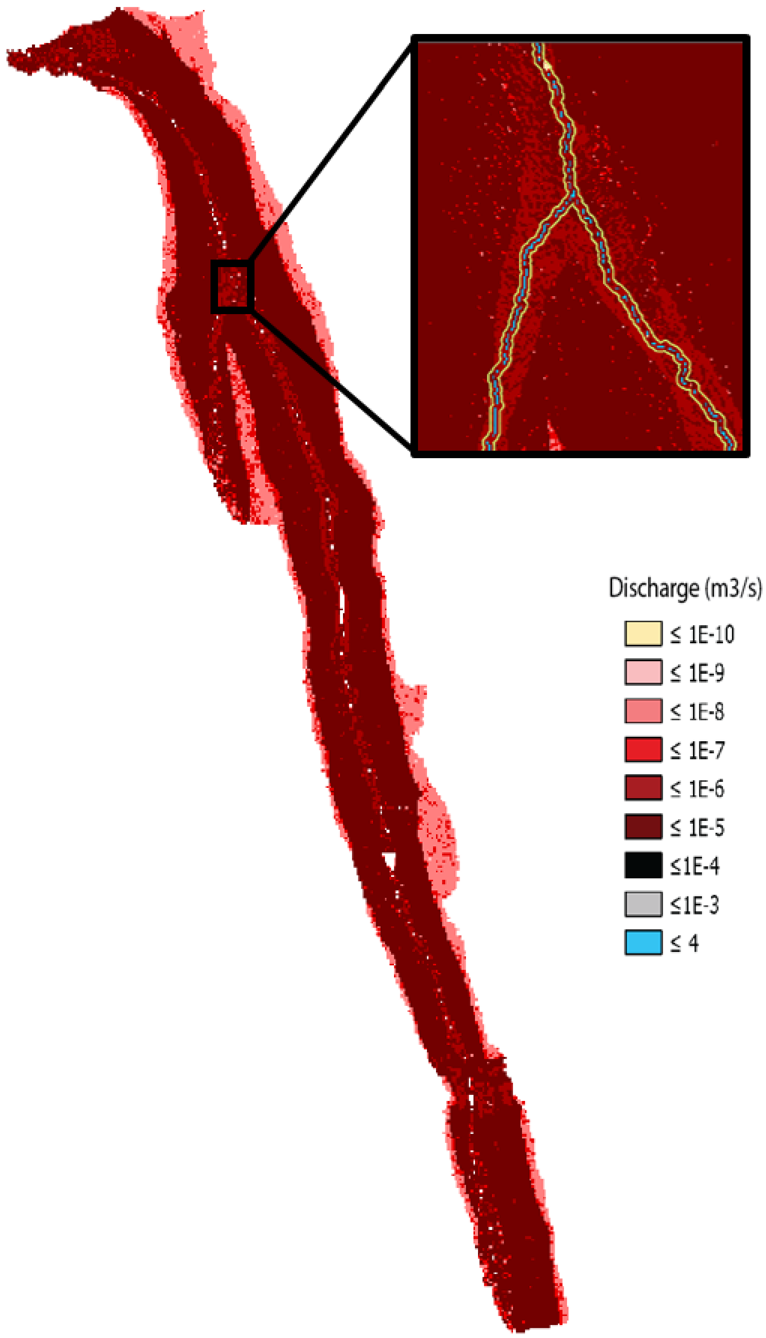

Figure 9. Magnitude raster is the final result of the Darcy Flow tool and apply some post calculations. Blow up section shows the buffer used to select the edges along the stream. Notice discharge values in the stream are much higher than elsewhere in the raster

Results

The culmination of all this spatial analysis resulted in a discharge flux of 5.65×10^{-3} m^3/s or 487.90 m^3/day. This represents the flux of every cell on either side of the stream at the moment in time the primary data was collected. Because the equations and tools calculated the values on a cell by cell basis, conservation of mass applies. During this time of season in Alaska, there was no precipitation and no overland flow. All the water entering the stream is assumed to be base flow. In order to compare this influx to the stream, I have hydrograph data from the same time the depth to the ice table and depth to the water table were measure(see Figure 10) The hydrograph is located at the pour point of the watershed, at the confluence of Imnavait Creek with the Kuparuk River(see Figure 1). With perfect conservation of mass the hydrograph data should match the number modeled by this ground water analysis. Hydrograph data was collected as a part Tyler King's thesis research at Utah State with Bethany Neilson.

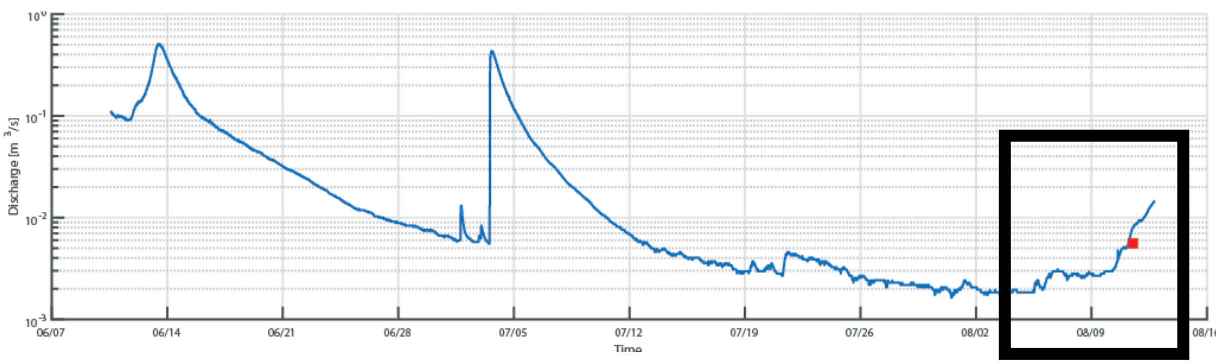

Figure 10 Hydrograph data from June to August of 2015. Box is around the week of 8/9/15. Red dot is my result of groundwater discharge into the steam as compare to the outflux of the stream.

Discussion

The active layer groundwater discharge flux I computed is extremely close to the observed same day. Using the observational data and characterization of hydraulic properties of a hillslope was very effective. The stratigraphy and terrain of this artic basin is extremely heterogeneous due to "microtopograpy", which refers to hummocks and polygonal features formed by season ice heaving and cryoturbation. The 5m DEM sufficiently represented the land surface and perhaps was just the right resolution to average out the microtopograpy.

As I continue to work on this project, I will perform a sensitivity analysis on the model identify and quantify the effects of using values +/- 1 standard deviation from the mean in each zone. Also I will decrease the raster resolution and see if that has any effect on the discharge flux.

This method would not be effective to predict or match stream output during times of overland flow or excessive precipitation as it has no way to account for anything other than groundwater. However it could be used to estimate base flow during that time. It could perhaps determine what contribution to the stream was coming from groundwater.

Conclusion

- This method of computing active layer groundwater flow is effective in times when all stream flow is base flow.
- Ignoring microtopography did not negatively affect the results of this computation.
- Using mean values of transmissivity was also effective.

References

Čapek, P., Diáková, K., Dickopp, J. E., Bárta, J., Wild, B., Schnecker, J., ... Hugelius, G. (2015). The effect of warming on the vulnerability of subducted organic carbon in arctic soils. *Soil Biology and Biochemistry*, *90*, 19-29.

Hinzman, L. D., Bettez, N. D., Bolton, W. R., Chapin, F. S., Dyurgerov, M. B., Fastie, C. L., ... Jensen, A. M. (2005). Evidence and implications of recent climate change in northern Alaska and other arctic regions. *Climatic Change, 72(3)*, 251-298.

Hinzman, L. D., & Kane, D. L. (1992). Potential response of an Arctic watershed during a period of global warming. *Journal of Geophysical Research: Atmospheres, 97(D3)*, 2811-2820.

Jorgenson, M. T., Shur, Y. L., & Pullman, E. R. (2006). Abrupt increase in permafrost degradation in Arctic Alaska. *Geophysical Research Letters, 33(2),* DOI:10.1029/2005GL024960. Add L02 whatever

Kane, D.L, Hinsman, L. D., Benson, C. & Everette, K. (1989). Hydrology of Imnavait Creek, an Arctic Watershed. *Holarctic Ecology, 12(3),* 262-269.

Kane, D. L., Hinzman, L. D., & Zarling, J. P. (1991). Thermal response of the active layer to climatic warming in a permafrost environment. *Cold Regions Science and Technology, 19(2),* 111-122.

Muskett, R. R., & Romanovsky, V. E. (2011). Alaskan permafrost groundwater storage changes derived from GRACE and ground measurements. *Remote Sensing*, *3(2),* 378-397.

Oechel, W. C., Vourlitis, G. L., Hastings, S. J., Zulueta, R. C., Hinzman, L. D., & Kane, D. L. (2000). Acclimation of ecosystem CO2 exchange in the Alaskan Arctic in response to decadal climate warming. *Nature*, *406(6799),* 978-981.

Osterkamp, T. E., & Romanovsky, V. E. (1999). Evidence for warming and thawing of discontinuous permafrost in Alaska. *Permafrost and Periglacial Processes*, *10(1),* 17-37.

Romanovsky, V. E., Smith, S. L., & Christiansen, H. H. (2010). Permafrost thermal state in the polar Northern Hemisphere during the international polar year 2007–2009: a synthesis. *Permafrost and Periglacial processes*, *21(2),* 106-116.

Schramm, I., Boike, J., Bolton, W. R., & Hinzman, L. D. (2007). Application of TopoFlow, a spatially distributed hydrological model, to the Imnavait Creek watershed, Alaska. *Journal of Geophysical Research: Biogeosciences, 112(G4)*

Schuur, E. A., Bockheim, J., Canadell, J. G., Euskirchen, E., Field, C. B., Goryachkin, S. V., ... & Mazhitova, G. (2008). Vulnerability of permafrost carbon to climate change: Implications for the global carbon cycle. *BioScience, 58(8)*, 701-714.

Shiklomanov, N. I., & Nelson, F. E. (2002). Active-layer mapping at regional scales: A 13-year spatial time series for the Kuparuk region, north-central Alaska. *Permafrost and Periglacial Processes, 13(3),* 219-230.

Walsh, J. E., Anisimov, O., Hagen, J. O. M., Jakobsson, T., Oerlemans, J., Prowse, T. D., ... Shiklomanov, I. (2005). Chapter 6: Cryosphere and hydrology. *Arctic Climate Impact Assessment*. Cambridge University Press (p.136-165).